IMPROVING GROUND MOTION SIMULATION CAPABILITIES FOR UNDERGROUND EXPLOSION MONITORING: COUPLING HYDRODYNAMIC-TO-SEISMIC SOLVERS AND STUDIES OF EMPLACEMENT CONDITIONS

Arthur J. Rodgers, Heming Xu, Ilya N. Lomov, N. Anders Petersson, Bjorn Sjogreen, Oleg Y. Vorobiev and Veraun Chipman

Lawrence Livermore National Laboratory

Sponsored by the National Nuclear Security Administration

Award No. DE-AC52-07NA27344/LL09-Simulation-NDD02

ABSTRACT

This project involves research being performed to improve ground motion simulation capabilities for underground explosion monitoring. We are working along two thrusts: 1) we are coupling hydrodynamic (non-linear shock) and seismic (linear anelastic) wave propagation codes; and 2) we are investigating the effect of source emplacement conditions on ground motions. For both thrusts we are modeling explosion motions using GEODYN, an Eulerian hydrodynamic code developed at Lawrence Livermore National Laboratory (LLNL). This code includes many important features for modeling shock waves in geologic materials, including non-linear response (e.g., effects of porosity, tensile failure, yielding) and adaptive mesh refinement. However, numerical solution of the hydrodynamic response is computationally expensive due to non-linear constitutive behavior, especially when compared to elastic wave propagation solvers. To propagate ground motions from the non-linear explosive source region to far-field seismic stations we are using a one-way coupling strategy to pass motions from GEODYN to WPP (LLNL's anelastic finite difference code for seismic wave modeling). Motions computed by GEODYN and recorded on a dense grid span the ranges where motions become linear (elastic). These are saved, processed and passed to WPP where they are introduced as a boundary source and continue to propagate as elastic waves at lower numerical cost than with GEODYN. In the past year we have worked on several important details to gain confidence that coupled GEODYN-to-WPP simulations are accurate. This involved modifying GEODYN to accurately model elastic surface waves. This is challenging because GEODYN uses hydrodynamic rather than elastodynamic equations of motions for the continuum. We have evaluated the handling of the free-surface by comparing GEODYN calculations to analytic solutions to Lamb's problem. We have evaluated the mechanics of passing motions from GEODYN-to-WPP by computing elastic solutions for a buried explosion with WPP, manipulating these motions as if they were computed by GEODYN and passing them to WPP and then comparing the solutions computed directly with WPP and passed from WPP-to-WPP. Excellent agreement was obtained. We have passed explosion generated motions computed with GEODYN to WPP and compared results to elastic solutions using a reduced displacement potential (RDP) approach and gotten excellent agreement with P-waves. In this case the near-field motions from GEODYN were analyzed to obtain an RDP and this was convolved with an elastic Green's function to model the response at longer range. Our second thrust of research involves parametric studies of normally buried explosions using different canonical geologic material models (e.g., granite, limestone, sandstone, tuff and alluvium). Simulations of explosion generated motions were analyzed to quantify the effects of emplacement conditions (material and depth of burial) on the elastic motions through the RDP.

OBJECTIVES

The objective of this project is to advance model capabilities for seismic motions generated by underground nuclear explosions (UNE's). Explosions generally involve the near instantaneous release of high temperature and pressure gas in a small volume of space. These high energy densities cause irreversible non-linear behavior in the surrounding material (rock) due to the generation and propagation of the outgoing hydrodynamic shock wave. It has been long appreciated that non-linear material response effects at the explosion emplacement have a strong impact on the long-range seismic motions (e.g., Werth and Herbst, 1963; Perret and Bass, 1975; Rodean, 1981; Murphy, 1981; Denny and Johnson, 1991). However, a full understanding of these effects has been difficult to obtain due to limitations in knowledge of detailed sub-surface three-dimensional (3D) structure and inadequate analytical or computational strategies to represent all relevant non-linear material response effects. Furthermore, the computational resources needed to accurately represent hydrodynamic phenomena from explosions require extremely fine temporal and spatial discretization, making it very difficult to calculate the hydrodynamic response for the scales required to compare with data. Advances in numerical methods and more powerful computational resources now make it possible to routinely compute the hydrodynamic response of earth materials to UNE's with ever improving fidelity.

This project seeks to improve capabilities for hydrodynamic modeling of UNE's. To this end we are working along two thrusts:

1. We are coupling our hydrodynamics code to our anelastic seismic wave propagation code to compute near-source shock-wave motions and propagate them to seismic distances.
2. We are performing series of parametric simulations to understand the impact of geologic material emplacement conditions on UNE ground motions and compare them to available source models.

RESEARCH ACCOMPLISHED

This project relies heavily on numerical simulation of the hydrodynamic response of earth materials to explosion loading. To model UNE's we are using GEODYN, a fully three-dimensional Eulerian hydrodynamic code developed at LLNL. This code incorporates many important features for modeling shock waves in geologic materials, including non-linear response (e.g. porosity, tensile failure, yielding), topography, gravity, 3D material heterogeneities. Importantly GEODYN uses adaptive mesh refinement to accurately represent the discontinuous shock wave front. GEODYN has been used on a wide range of problems involving high-energy loading of earth materials (Antoun et al., 2001, 2004; Antoun and Lomov, 2003; Lomov et al., 2003). GEODYN includes material models accounting for the effects of porous compaction and dilation, material strength hardening and softening as well as scale and rate-dependence (Rubin et al., 2000; Vorobiev et al., 2007; Vorobiev, 2008). It was shown in previous studies (Vorobiev et al. 2000) that the strength model used in calculations has a great effect on both the shape and the amplitude of the forming waves at the ranges where the elastic-plastic flow takes place. The model used ultimately defines the elastic radius and the duration of the pulse at this radius. For most of the calculations shown in this report we ran GEODYN in axisymmetric two-dimensional (2D) mode. All simulations in this report are fully tamped, that is the explosive is buried and is in contact with the surrounding rock.

For seismic (weakly anelastic) motions we use WPP, a Carestian finite difference code developed at LLNL materials (Nilsson et al., 2007). WPP includes mesh refinement to increase the grid spacing as seismic wavespeeds increase with depth and free-surface topography (Appelo and Petersson, 2008; Petersson and Sjogreen, 2009, 2010; Sjogreen and Petersson, 2010). WPP has been used for modeling moderate and scenario earthquake ground motions in the San Francisco Bay area (Aagaard et al., 2008, 2010; Rodgers et. al, 2008) and the effects of surface topography on explosion ground motions (Rodgers et al., 2010). WPP is an open-source computer program with extensive documentation (Petersson and Sjogreen, 2011) and examples and is freely available (Petersson, 2011).

Evaluation of GEODYN Solutions and Coupling to WPP

We chose a homogeneous half-space as a numerical model to test the GEODYN's computational scheme. We examined two kinds of elastic (linear) sources: vertical force (Lamb's problem) and dilatational volume source

simulating an explosion. Analytical solutions are obtained for both kinds of sources (Luco and Aspel, 1983). For the vertical force, the source time function is a Ricker function with a peak frequency of 8 Hz. Numerical results from GEODYN are plotted against the analytical solutions for a point on the free surface at 1 km range (Figure 1, left). Analytical solutions are plotted as solid lines and the numerical solutions as dashed lines. It is seen that the surface waves dominate for this source at this range. The agreement of the exact solutions and numerical solutions is excellent for body waves, but there is some mismatch for Rayleigh waves in phase and amplitude. Since GEODYN relies on an Eulerian scheme, the free surface is not a clear interface between rock and air, and wave motion results in mixed cells of air and solid earth. The surface wave is very sensitive to the treatment of the free surface boundary. In this case, the imperfect implementation of the free surface might result in some energy leakage into the air above the free surface (Graves, 1996).

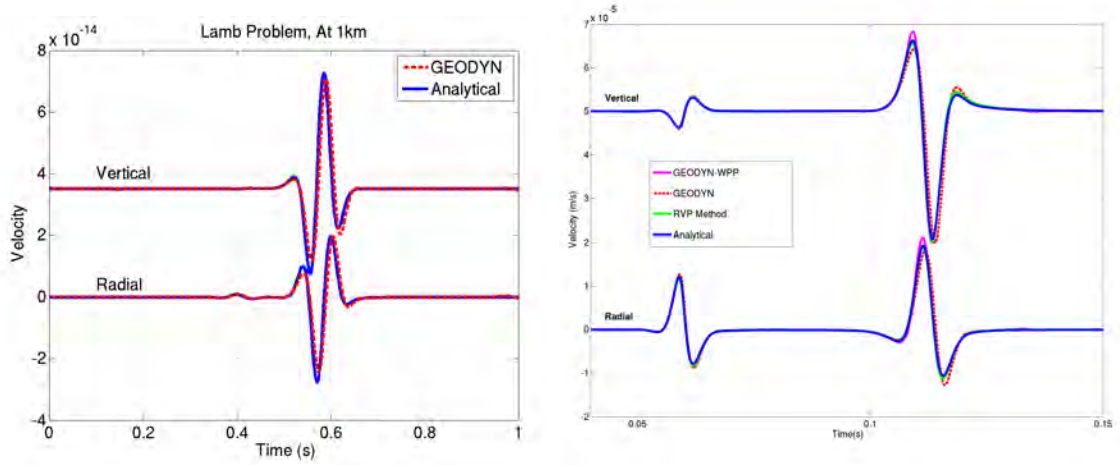

Figure 1. Benchmark tests in linear elastic medium. The top and bottom traces represent vertical and radial component velocities, respectively. (left) Lamb's problem: GEODYN (red dashed) and analytical (blue solid) solutions. (right) Dilatational volume source problem: analytical solution (solid blue), semi-analytical solution using the numerically derived reduced velocity potential (solid green), direct GEODYN calculation (red dashed lines) and the WPP solutions with GEODYN solutions coupled as driving boundary conditions (solid magenta).

For a dilatational volume source at a depth of 10 m we compare numerical solutions with GEODYN and analytical solutions at an offset 360 m on the surface. The material model is granite with a P-wavespeed of 6 km/s. All solutions were low-pass filtered below 150 Hz. The results are shown on the Figure 1 (right). It is evident that an explosion source excites stronger body waves (relative to the Rayleigh waves) than Lamb's problem. Again we see there is an excellent agreement between the GEODYN numerical solution (red dashed) and analytical solution (blue solid) for body waves and some mismatch for Rayleigh waves at the same location, presumably due to free-surface boundary condition effects as in Lamb's problem (above). In addition, for this type of volume source, the reduced velocity potential (RVP) (Murphy, 1991) is conveniently derived in the linear elastic region from the GEODYN calculation then convolved with the dilatational volume source. These semi-analytical solutions are plotted as green lines and they are also in good agreement with the analytical solutions. This serves an additional check that GEODYN yields accurate spherical waves for calculating the RVP. Furthermore, we use the coupling strategy described above to propagate GEODYN's solution from the elastic region to the same station location using WPP (magenta lines Figure 1, right). It is seen that the body waves calculated by the coupling method match well with the analytical solutions and Rayleigh waves are in phase with the analytical solutions but the amplitudes show some differences from the analytical solutions. Again it is likely attributable to the imperfect free surface implementation in the numerical scheme. As an additional validation on the coupling scheme, we use WPP instead of GEODYN to calculate the near source wavefield in a linear elastic medium and use the same strategy as above, to propagate the near source solutions to distance. The comparison between the direct WPP solution and the WPP-to-WPP solution is in excellent agreement in form of body wave and surface waves (not shown in Figure 1).

Nonlinear wave propagation

Consider a 1 kt chemical explosion at a depth of 10 m in nonlinear material with a porosity of 2% in a half-space. The stress-strain relationship is nonlinear and bulking is included. As above we calculate wave propagation due to the explosion source with GEODYN and also use the coupling strategy to propagate the GEODYN solutions beyond the elastic radius to distance with WPP. For this problem no analytical solutions are available. We compared the direct GEODYN solutions with the WPP solutions in order to further validate the accuracy of the GEODYN calculations and the coupling strategy for the nonlinear source problem.

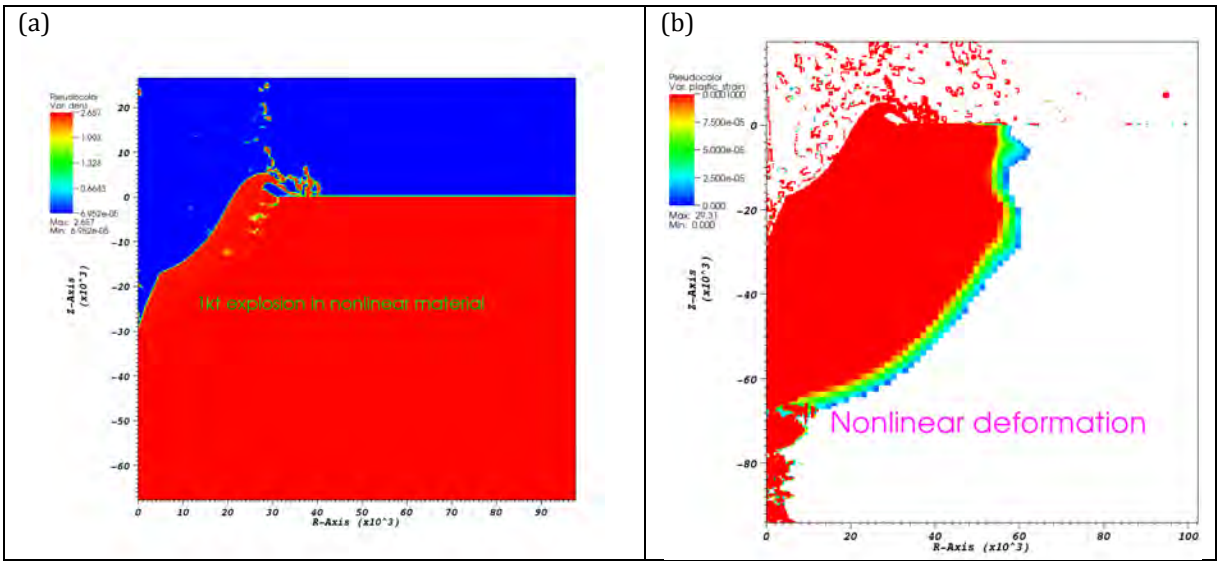

Figure 2. Explosion-induced crater formation (a) and nonlinear deformation (right). The unit of the axes is mm. The free surface is at z=0. The explosion is centered at a depth of 10 m. The crater formed by a 1 kt chemical explosion is about 30 m deep and 30 m horizontally and the nonlinear deformation extent is about 60 m.

Figure 2(a) shows the material distribution after the explosion. The red part denotes solid materials and blue part denotes air. The near-surface explosion vaporizes the surface material, and bursts produce a shallow depression to form a crater deep to 30 m and extended to 30 m on the surface. Figure 2(b) shows the incurred non-linear deformation region (plastic deformation > 1%) which is not spherically symmetric; it extends to about 60m horizontally and vertically. The numerical GEODYN solutions are saved at the locations beyond the non-linear deformation region, filtered up to 30 Hz (lower than the corner frequency) and passed to WPP as a boundary driving condition.

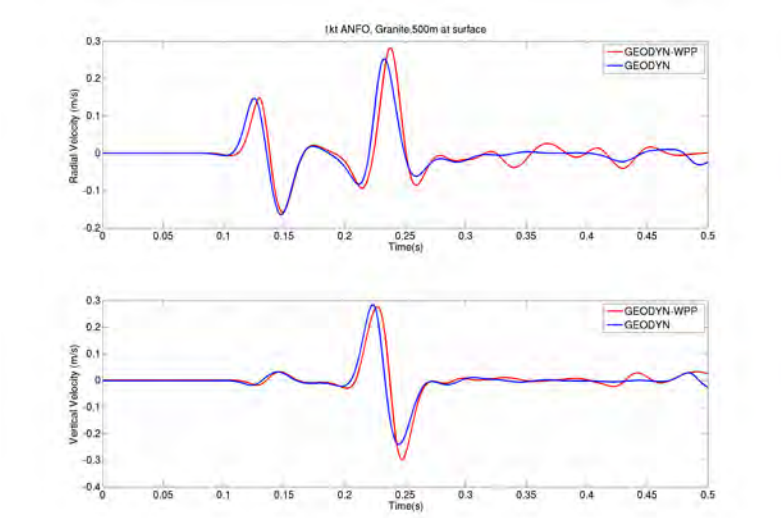

Figure 3. Comparison of the direct GEODYN solutions (blue curves) and WPP solutions (red curves) coupled with GEODYN solutions. The top is the radial component and bottom the vertical component. All solutions are filtered up to 30Hz which is lower than the corner frequency. The agreement of the two solutions is evident in form of the body wave and Rayleigh wave phases.

Figure 3 shows the comparison of the direct GEODYN solutions (blue curve) and the WPP solutions (red curve) at an offset of 500m on the free surface for the 1 kt chemical blast. The top plot is the radial component and the bottom vertical component. All the waveforms are filtered up to 30Hz (below the corner frequency). The agreement of the two solutions in form of the P, S and Rayleigh amplitudes and phases is fairly good - the coupled WPP solutions are slightly late, probably resulting from the slight discrepancy between elasticity in WPP and poroelasticity in GEODYN for this porous material. The motion at late times is probably due to the imperfect outflow boundary conditions for the small volume used in these simulations.

Parametric studies of emplacement conditions

The source time function for explosions depends on the material properties, depth, yield as well as differences in nuclear versus chemical explosion loading. The Mueller-Murphy explosion source model (Mueller and Murphy, 1971; Stevens and Day, 1985) provides a parametric representation of the P-wave radiation spectrum from a nuclear explosion as a function of yield and depth-of-burial with empirical parameters for various geologic materials (granite, salt, shale and tuff). The parameters for other materials are not determined, probably due to a lack of sufficient explosion data. In this study we perform a series of parametric studies on the source spectra from a variety of yields and geological materials in order to investigate the characteristics of the sources in different materials, including hard rock (granite) and porous rock (weathered granite, sandstone). GEODYN allows us to introduce explosion loading in different ways that can mimic the rapid energy deposition of a nuclear explosion or the slower burn of a chemical (high-explosives, such as ammonium nitrate and fuel oil, ANFO) blast. In these simulations all explosions are fully tamped.

The yields used in the GEODYN calculations range from 0.5 kt to 5 kt for nuclear explosions and only 1 kt for chemical explosion to compare with the nuclear explosion of the same yield. All the explosions are normally buried fully and contained underground (DOB=122 m/kt$^{1/3}$, e.g. Stevens and Day, 1985). Gravity and lithostatic pressure is included. The granite model is the hard rock model obtained from modeling near-field motions from the PILEDRIVER explosion (Antoun et al, 2001), weathered granite model represents a weaker hard rock (Sierra White granite) and sandstone model is developed for porous Berea sandstone (Vorobiev, 2008). Figure 4 shows examples of the permanent nonlinear deformation (damage) for the nuclear explosions of 1 kt (left) and 5 kt (right) in the hard rock. The nonlinear deformation region extends to 300 m and 500 m on the surface for 1 kt and 5 kt respectively and the region are clearly not spherically symmetric.

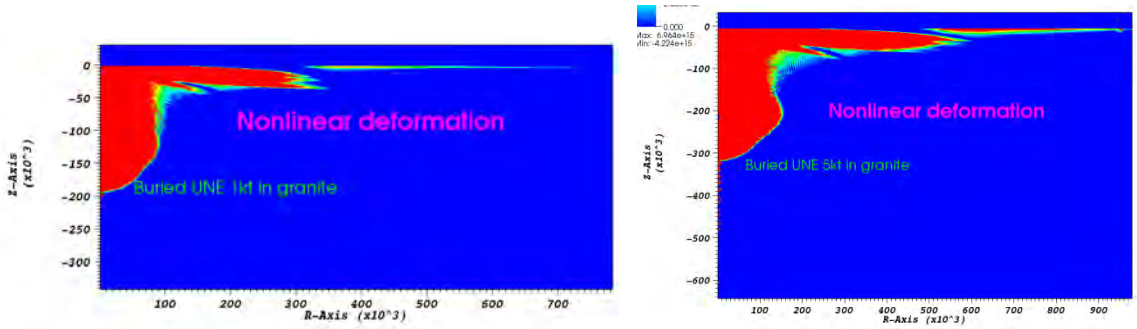

Figure 4. Nonlinear region extents (red) for normally buried nuclear 1kt (left) and 5kt (right) explosions. The unit of the coordinate axes is millimeters (mm). Note the non-linear (damaged) regions are not spherically symmetric.

The source spectra are derived from the radial-component seismograms recorded beyond the elastic radius at the source level. The reduced velocity potential (RVP, Ψ_∞) is estimated from the seismogram in the time domain and then the low-frequency source spectral level (seismic moment) is defined by $4\pi\rho\alpha^2\Psi_\infty$ (Stevens and Day, 1985) where α is P wave speed, ρ is density and Ψ_∞ is the value of the RVP at long times, proportional to the permanent deformation near the source. Figure 5 shows the derived source spectra for the nuclear explosions (0.5, 1, 2, 3, 4, 5 kt) and 1 kt chemical explosion (blue dashed line). The red dashed line is the MM71 source model. It is evident that the spectrum for the GEODYN computed motions for 1 kt nuclear blast agrees very well with the MM71 spectrum in amplitude, although the corner frequency is slight higher for the granite model we used. It is found that the 1 kt chemical explosion has twice the low-frequency spectral level (moment) of the corresponding nuclear explosion, illustrating the higher efficiency of transferring energy into rock for slower burning chemical explosions. For nuclear explosions in such hard granite, it appears that the nuclear source strength is proportional to the yield, and the corner frequency decreases with yield from 4 Hz for 0.5 kt to 2 Hz for 5 kt consistent with Denny and Johnson (1991).

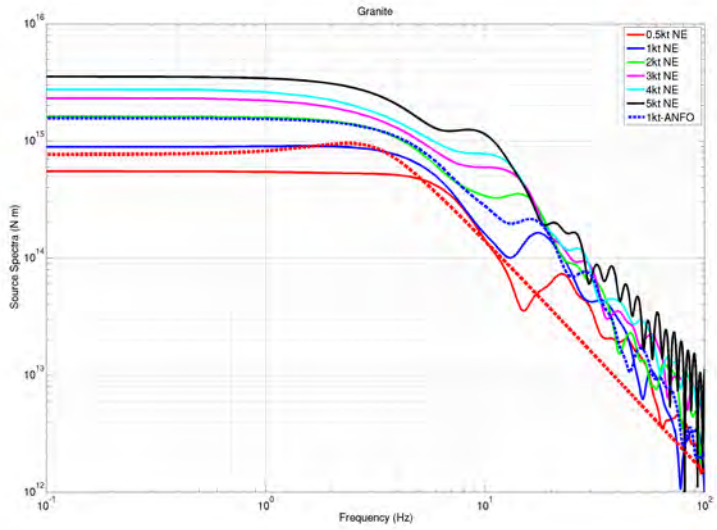

Figure 5. Source spectra for explosions in hard granite. The yields range from 0.5-5 kt. The red dashed line is the Mueller-Murphy source model for a 1 kt nuclear explosion and is consistent with the calculated spectrum derived from the GEODYN's calculations. The dashed blue line is the 1 kt chemical (ANFO) source and is about double that for a 1 kt nuclear explosion (solid blue).

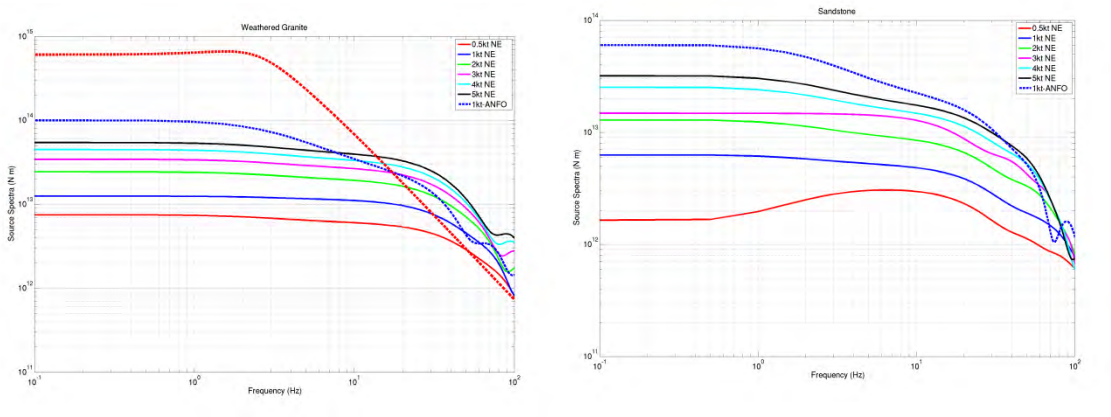

Figure 6. Similar to Figure 5 but for a weathered granite model (left) and porous sandstone model (right). It is noted that the source strengths are greatly reduced and corner frequencies are increased relative to Figure 5. The red dashed line on the left figure is the MM71 source model for granite.

Figure 6 shows the source spectra for the weak materials: weathered granite on the left and sandstone on the right. The red dashed line on the left is the MM71 source model (1 kt nuclear) and the blue dashed lines is the computed source spectrum for 1 kt chemical (ANFO) explosion. It is seen that all the source strengths are reduced by a factor of more than ten (10) relative to the granite and the corner frequencies accordingly increase above those for granite material. Similar variability for soft materials such as alluvium, is also seen in the results by Denny and Johnson (1991). While the source strengths appear proportional with the yield in weathered granite, an irregularity is clearly seen for explosions in the sandstone model, which are likely related to rock behavior at higher porosity. For both weak material models the chemical explosion transfers much more energy into the surroundings relative to the nuclear explosion of the same yield than for the hard, imporous granite in which the factor is nearly 2.

CONCLUSIONS AND RECOMMENDATIONS

We report improvements in the simulation of explosion generated ground motions for chemical and nuclear explosions using GEODYN, a three-dimensional Eulerian hydrodynamics code capable of incorporating nonlinear material properties, topography and heterogeneities. Due to the intensive computational requirements, the near source wavefields need to be propagated by using coupling to a faster linear anelastic code, WPP, to distances at which seismic measurements would be made. The accuracy of GEODYN in modeling free surface effects is benchmarked against the analytical solutions in the linear elastic medium. The accuracy of the coupling scheme from GEODYN to WPP is also benchmarked by comparing the solutions computed directly by GEODYN. The mechanics of coupling is verified by passing WPP elastic motions to WPP using the GEODYN-to-WPP one-way coupling scheme.

GEODYN is used to investigate the source characteristics in different geologic material conditions from hard granite to porous sandstone. GEODYN allows calculation of the permanent deformation and material damage. We show that material damage extends above and outward from the source. Simulations of geologic material dependence show that the explosion source strengths in hard, low porosity granite are consistent with the empirical Mueller-Murphy source model (Mueller and Murphy, 1971; Stevens and Day, 1985) and consistent with others reports (Denny and Johnson, 1991). A chemical explosion in granite appears to show twice the P-wave radiation amplitude as a nuclear explosion of the same yield, however much larger amplifications of seismic radiation (chemical vs. nuclear) are seen in porous materials. For porous materials such as sandstone with a porosity of 20%, the source strengths are greatly reduced relative to explosions in granite at the same yield, due to the strong hysteretic behavior of the material that causes significant energy dissipation.

The simulation of underground explosions (chemical and nuclear) using more complete physics represented in hydrodynamic numerical codes holds great promise to improve understanding of the seismic radiation emerging from explosions. The inclusion of non-linear material properties reveals great sensitivity of seismic radiation to geologic material at the source, as well as yield and depth-of-burial effects. This type of modeling is made possible

with advances in high-performance computing and improvements in numerical methods to represent non-linear material response. Further study along this line of research may provide important insights into the dependence of seismic radiation with emplacement conditions.

ACKNOWLEDGEMENTS

Simulations were performed on the SIERRA Linux cluster operated by Livermore Computing. We are grateful for access to these facilities through the Grand Challenge Allocation.

REFERENCES

Aagaard, B., T. Brocher, D. Dreger, A. Frankel, R. Graves, S. Harmsen, S. Larsen, K. McCandless, S. Nilsson, N.A. Petersson, A. Rodgers, B. Sjogreen and M. L. Zoback (2008). Ground motion modeling of the 1906 SanFrancisco earthquake II: Ground motion estimates for the 1906 earthquake and scenario events, *Bull. Seismol. Soc. Am.* 98**:** 1012–1046, doi: 10.1785/0120060410.

Aagaard, B. T., R. W. Graves, A. Rodgers, T. M. Brocher, R. W. Simpson, D. Dreger, N. A. Petersson, S. C. Larsen and S. Ma (2010). Ground motion modeling of Hayward fault scenario earthquakes II: Simulation of long period and broadband ground motions, *Bull. Seismol. Soc. Am.* 100: 2945–2977.

Antoun, T. H., I. N. Lomov, and L. A. Glenn (2001). Development and application of a strength and damage model for rock under dynamic loading, in proceedings of the 38th U.S. Rock Mechanics Symposium, Rock Mechanics in the National Interest, D. Elsworth, J. Tinucci and K. Heasley (eds.), A. A. Balkema Publishers, Lisse, The Netherlands, 369–374.

Antoun, T. H. and I. N. Lomov (2003). Simulation of a spherical wave experiment in marble using multidirectional damage model, 13th American Physical Society Topical Conference on Shock Compression of Condensed Matter, Portland, OR July 20–25, 2003.

Antoun, T. H., I. N. Lomov and L.A. Glenn (2004). Simulation of the penetration of a sequence of bombs into granitic rock, *Int. J. Impact Eng.* 29: 81–94.

Appelo, D. and N.A. Petersson (2008). A stable finite difference method for the elastic wave equation on complex geometries with free surfaces, *Comm. Comput. Phys*. 5: 84–107.

Denny, M.D and L. R. Johnson (1991). The explosion seismic source function: models and scaling laws reviewed, Explosion Source Phenomenology, pp1-24, Eds. S. R Taylor, H. J Patton and P.G Richards, *Geophysical Monograph*, 65.

Graves, R.W. (1996). Simulating seismic wave propagation in 3D elastic media using staggered-grid finite difference, *Bull. Seismol. Soc. Am*. 86:1091–1106.

Lomov. I. N., T. H. Antoun, J. Wagoner and J. Rambo (2003). Three-dimensional simulation of the Baneberry nuclear event, in Proceedings of the 13th American Physical Society Topical Conference on Shock Compression of Condensed Matter, Portland, OR July 20–25, 2003.

Luco, J.E and R.J. Apsel (1983). On the Green's functions for a layered half-space. Part I, *Bull. Seismol. Soc. Am*. 73: 909–929.

Mueller, R. and J. Murphy (1971). Seismic characteristics f\of underground nuclear detonations Part 1: Seismic source scaling, *Bull. Seismol. Soc. Am*. 61: 1675–1692.

Murphy, J. (1981). P wave coupling of underground explosions in various geologic media, in *Identification of Seismic source – Earthquake or Explosion*, E. S. Husebye and S. Mykkelveit (eds.), 201–205.

Nilsson, S., N.A. Petersson, B. Sjogreen, H.-O. Kreiss (2007). Stable difference approximations for the elastic wave equation in second order formulation, *SIAM J. Numer. Anal*. 45: 1902–1936.

Perret W. R. and Bass R. C. (1975). Free-field ground motion induced by underground explosions, Sandia National LaboratoryReport No. SAND74-0252.

Petersson, N. A. (2011). WPP software website, https://computation.llnl.gov/casc/serpentine/software.html

Petersson, N. A. and B. Sjögreen (2009). An Energy Absorbing Far-Field Boundary Condition for the Elastic Wave Equation, *Comm. Comput. Phys*. 6: 483–508.

Petersson, N. A. and B. Sjögreen (2010). Stable and efficient modeling of anelastic attenuation in seismic waves, submitted to *Comm. Comput. Phys*, LLNL-JRNL-460239.

Petersson, N. A. and B. Sjögreen (2011). User's guide to WPP version 2.1, Lawrence Livermore National Laboratory technical report, LLNL-SM-487431.

Rodean, H (1981). Inelastic prcesses in seismic wave generation by underground explosions, in *Identification of Seismic source – Earthquake or Explosion*, E. S. Husebye and S. Mykkelveit (eds.), p. 97–189.

Rodgers, A., N. A. Petersson, and B. Sjögreen (2010). Efficient generation of shear waves from shallow explosions by topographic scattering near the North Korean nuclear test site, *J. Geophys. Res.* 115: B11309, doi:10.1029/2010JB007707..

Rubin, M. B., O. Vorobiev, and L. A. Glenn (2000). Mechanical and numerical modeling of a porous elastic viscoelastic material with tensile failure, *Int. J. Solids and Structure* 37: 1841–1871.

Sjögreen, B. and N. A. Petersson (2010). Stable grid refinement and singular source discretization for seismic wave simulations, *Comm. Comput. Phys*, LLNL-JRNL-419382.

Stevens, J. L and S. M. Day (1985). The physical basis of mb:Ms and variable frequency magnitude methods for earthquake/explosion discrimination, *J. Geophy. Res*. 90: 3009–3020.

Vorobiev O. Y., T. Antoun, I. N. Lomov, L. A. Glenn (2000). A strength and damage model for rock under dynamic loading, *Proceedings of the 11th American Physical Society Topical Conference on Shock Compression of Condensed Matter*, Snowbird, UT, 1999, Michael D. Furnish and Lalit C. Chhabildas and Robert S. Hixson (eds.)

Vorobiev O. Yu, Liu B. T, Lomov I.N, Tarabay T. H (2007) Simulation of penetration into porous geologic media, *Int. J. of Impact Eng* 34: 721–731

Vorobiev, O. (2008). Generic strength model for dry jointed rock masses, *Int. J. of Plasticity* 24: 2221–2247.

Werth, G. and R. Herst (1963). Comparison of amplitudes of seismic waves from nuclear explosions in four mediums, *J. Geophys. Res*. 68: 1463–1475.